APPLICATION OF VORONOI DIAGRAM TO MASK-BASED INTERCEPTING PHASE-SPACE MEASUREMENTS

A. Halavanau[1,2*], G. Ha[3], P. Piot[1,2], E. Wisniewski[4], Q. Gao[5], J. Power[4]
[1] Department of Physics and Northern Illinois Center for Accelerator & Detector Development, Northern Illinois University DeKalb, IL 60115, USA
[2] Fermi National Accelerator Laboratory, Batavia IL 60510, USA
[3] POSTECH, Pohang, Kyoungbuk, 37673, Korea
[4] Argonne Wakefield Accelerator, Argonne National Laboratory, Lemont, IL, 60439, USA
[5] Accelerator laboratory, Department of Engineering Physics, Tsinghua University, Beijing, China

Abstract

Intercepting multi-aperture masks (e.g. pepper pot or multislit mask) combined with a downstream transverse-density diagnostics (e.g. based on optical transition radiation or employing scintillating media) are commonly used for characterizing the phase space of charged particle beams and the associated emittances. The required data analysis relies on precise calculation of the RMS sizes and positions of the beamlets originated from the mask which drifted up to the analyzing diagnostics. Voronoi diagram is an efficient method for splitting a plane into subsets according to the distances between given vortices. The application of the method to analyze data from pepper pot and multislit mask based measurement is validated via numerical simulation and applied to experimental data acquired at the Argonne Wakefield Accelerator (AWA) facility. We also discuss the application of the Voronoi diagrams to quantify transversely-modulated beams distortion.

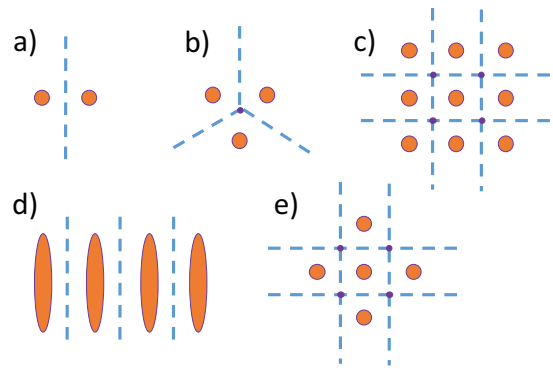

Figure 1: Examples of Voronoi diagrams drawn for different arrangements of initial points. a) and b) demonstrate the principle of a diagram, c) - e) display diagrams for most common tungsten mask configurations.

INTRODUCTION

Voronoi diagram is a method of dividing a plane into subsets with bisectors drawn between given points. It was proposed by G. Voronoi in 1908 [1] and since then has been employed in various fields of Science and Industry, e.g. in image segmentation, tessellation algorithms, computational geometry problems [2]. In Beam Physics this method can benefit to charged particle beams phase-space analysis and PIC codes improvement [3].

To illustrate the process of drawing Voronoi diagram, consider a set of points arranged in (x, y)-plane; see orange circles Fig. 1. First, a pair of neighboring points is connected with a line segment and a perpendicular bisector is drawn onto that segment. When bisectors from different segments intersect, they form a Voronoi vortex (intersection point), and Voronoi cells -convex or concave polygons, depending on the number of original points and its position on the diagram; see Fig. 1. Note, that for the case of perfectly grid-lined point formation each cell (excluding edge cells) will have exactly four vortices and a rectangular shape with the side equal to the spacing between points. When distortion is introduced to such formation, the cells become convex polygons, thus as a measure of the distortion the average cell area can be used. Since each cell contains a point of interest in its geometric center, the (x, y)-plane is automatically segmented into regions of interest which can be independently considered for further analysis.

APPLICATION IN SLIT/MASK BASED EMITTANCE MEASUREMENT

One of the most common methods of measuring charged particles beam emittance is an intercepting tungsten mask or slit. The mask is followed by transverse-density diagnostics (typically a scintillating screen) where the bunch-let formation is observed; see Fig. 2. The resulting emittance $\epsilon_{rms}^2 =< x^2 >< x'^2 > - < x'x >^2$ is deduced from known parameters of the mask (size d, pitch p), beam size at the mask, distance to the screen L and measured RMS size of each bunch-let [4]. Circular masks of cross- and grid-shape were manufactured and used for 4D emittance measurements at AWA facility [5, 6]. The main purpose of this paper is to amend these studies with a new emittance calculation algorithm, described below.

In a first step, all the beamlets are located via 2D peak finding algorithm and initial Voronoi diagram is generated; see Fig. 3. The edge polygons are discarded based on the intensity threshold, and given patch [Fig. 3 (b)] is further re-

* ahalavanau@niu.edu

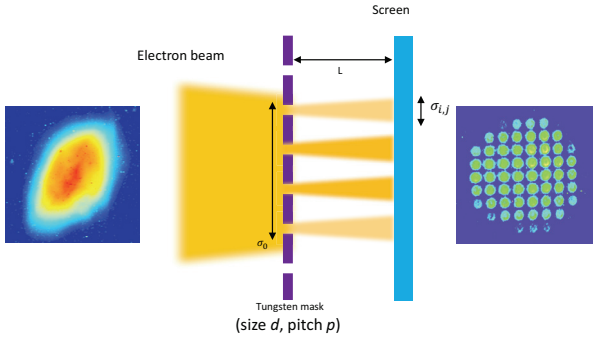

Figure 2: Schematics of the pepper pot emittance measurement technique. Electron beam (left inset) is propagated through the tungsten mask with periodic perforation in (x, y)-plane and resulting bunch-lets are recorded at the screen downstream of the mask (right inset).

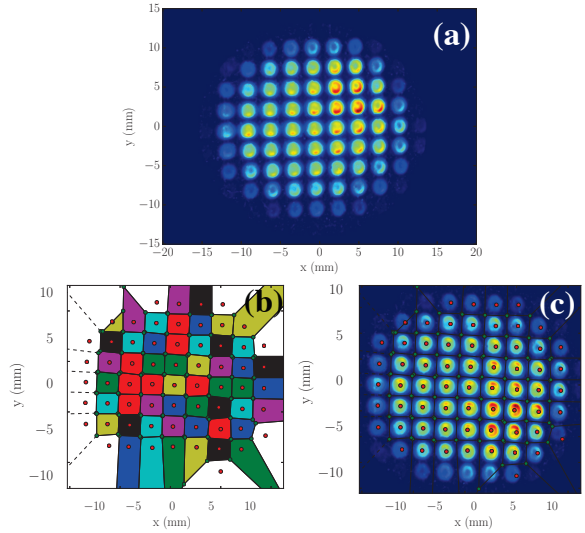

Figure 3: Demonstration of Voronoi mesh generation for emittance measurement. (a) Original pepper-pot segmented beam image. (b) and (c) Patches for separate beamlets (randomly colored) and masked beam image respectively.

analyzed. As it can be seen on Fig. 3, some beamlets appear to have peculiar hot spots away from its center, therefore distorting the Voronoi diagram. To alleviate this problem, a statistical center-of-mass calculation is done to refine the beamlet coordinates and therefore ensure the mesh is equally sparse with each patch containing only one beamlet; see Fig. 3 (c).

After the mesh refinement, statistical RMS values of σ_x, σ_y and beamlet relative positions are computed. The resulting value of the emittance can be deduced from well-known formula [4]:

$$\epsilon_{rms}^2 \approx \frac{1}{N^2}\left(\left[\sum_{j=1}^{m} n_j(x_{sj}-\bar{x})^2\right]\left[\sum_{j=1}^{m}\left(n_j\frac{\sigma_j^2}{L^2}+n_j(\bar{x_j'}-\bar{x'})^2\right)\right] - \left[\sum_{j=1}^{m} n_j x_{sj}\bar{x_j'} - N\bar{x}\bar{x'}\right]^2\right),$$

where N - total number of particles (integrated intensity of the region of interest), n_j - number of particles traveled through j-th slit (j-th beamlet intensity), m - total number of beamlets analyzed, $\bar{x}$ - mean position of all beamlets, $\bar{x'}$ - mean divergence of all beamlets, σ_j - RMS size of the beamlet, x_{sj} - j-th beamlet position, L - distance between mask and screen.

More densely perforated masks provide better statistical probe of the beam phase space, however, it increases the complexity of the bunch-let formation image analysis. The Voronoi diagram method can serve as fast and yet simple method of image segmentation. The mesh generation procedure is easily accessible via PYTHON-SCIPY package.

AWA-DBA ELECTRON BEAM MEASUREMENTS

AWA "drive-beam" accelerator (AWA-DBA) diagrammed in Fig. 4. In brief, the UV laser pulse hits a high-quantum efficiency Cesium Telluride (Cs_2Te) cathode located in a L-band (1.3-GHz) RF gun to produce 7 MeV electron bunch. The electron bunches are then further accelerated in an L-band normal conducting cavities up to 75 MeV. Several YAG:Ce scintillating screen (YAG in Fig. 4) are available to measure the beam transverse density along the accelerator beamline. For a detailed description of the facility the reader is referred to Ref. [7].

To perform pepper-pot emittance measurement procedure, 9 micron circular mask was inserted at the slit location on Fig. 4. 1 nC 48 MeV electron beam was then propagated through the mask and the electron distribution was registered at the YAG6 location downstream of the mask. None of the electron emittance, perforation spacing and screen location optimization procedures were applied prior to the experiment, however the acquired data gives a good test case for debugging and testing. The resulting measured normalized emittance values are ϵ_x=6.5 μm±0.7 μm and ϵ_y=7.2 μm ±0.9 μm for horizontal and vertical planes respectively. Further development of the technique will be made in the future.

TRANSVERSE MODULATION ANALYSIS

The Voronoi diagram segmentation method can also be applied for beam image transverse modulation analysis. Recently a laser transverse modulation technique was implemented at AWA using microlens arrays (MLAs). A detailed explanation of the MLA laser shaping technique is available in Ref. [8].

We started with a laser distribution pictured on Fig. 5 and propagated modulated electron beams to YAG1 location. To analyze the mean distortion of the electron beamlet pattern due to collective beam dynamics effects, we generated a Voronoi diagram and computed the mean area of the beamlet

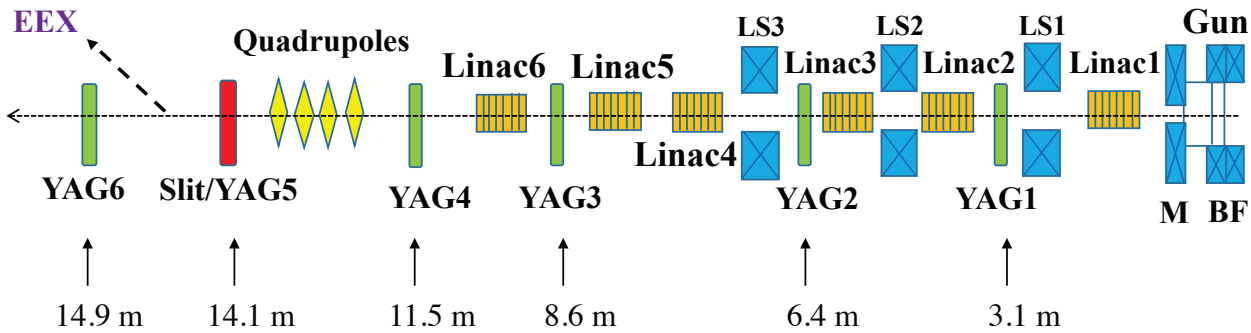

Figure 4: Overview of the AWA-DBA beamline only showing elements relevant to the performed experiment. Bucking-focusing (BF) and matching (M) solenoids were adjusted to image the beam on YAG screens. Linac solenoids (LS) and quadrupoles were turned off during the experiment. The positions of the YAG viewers are denoted in meters. The energy gain of one accelerating cavity (linac) is 10 MeV. EEX label marks the separate double-dogleg beamline for emittance exchange experiments.

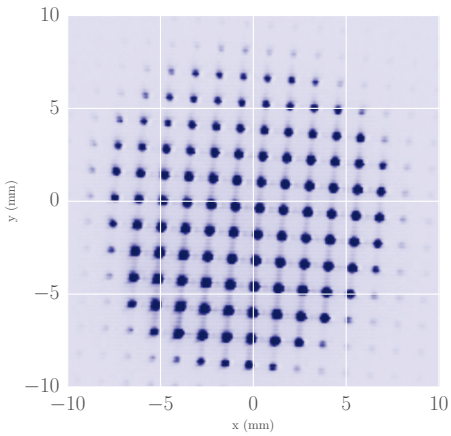

Figure 5: MLA UV-laser shaped spot with beamlet formation used in the experiment.

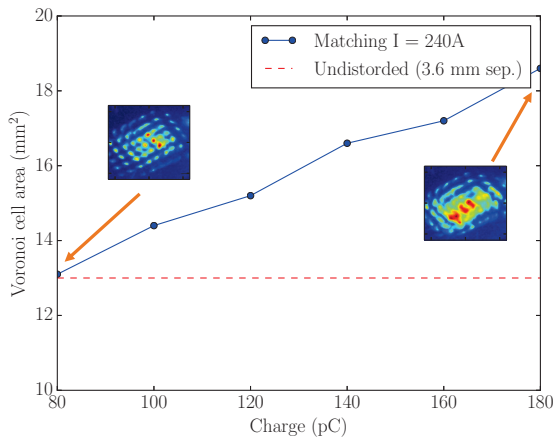

Figure 6: Average Voronoi cell area for matching solenoid current 240A as a function of charge. The insets demonstrate the electron beam pattern distortion due to collective beam dynamics effects. The dashed line corresponds to the separation of the beamlets of 3.6 mm at Q = 60 pC.

surrounding polygons. Multi-beam formation was obtained first at Q=60 pC and matching solenoid current I=240 A. As the charge was increased, the original well-defined pattern [Fig. 6, left inset] became distorted, resulting in smeared formation [Fig. 6, right inset] and rapidly growing average Voronoi cell area Such procedure can be complimentary to 2D FFT analysis of the image (e.g. bunching factor calculation), by taking into account separate beamlets shape, and not the multi-beam formation as a whole.

Note that in pepper-pot emittance measurement and in multi-beam pattern analysis Voronoi diagram remains independent of image rotation angle, which is an advantage in comparison to simple grid-like image segmentation.

CONCLUSIONS

We demonstrated the potential applications of Voronoi diagram technique in electron beam emittance measurement. Such a method can improve the accuracy of the measurement by better handling of densely perforated masks. The technique can be also applied for transverse modulation beam image analysis. The application of Voronoi diagrams in Beam Physics are not limited to the discussed examples and more studies will be conducted in the future.

ACKNOWLEDGMENTS

AH is thankful to V. Khodygo (Aberystwyth University, UK) for in-depth discussions about Voronoi diagrams.

REFERENCES

[1] G. Voronoi. *J. Reine Angew. Math*, vol. 134, pp. 198-287, 1908.

[2] F. Aurenhammer. *ACM Comput. Surv.*, vol. 23(3), pp. 345-405, 1991.

[3] Phuc T. Luu, T. Tuckmantel, and A. Pukhov, *Computer Physics Communications*, vol. 202, pp. 165-174, 2016.

[4] Min Zhang, report FERMILAB-TM-1988, 1996.

[5] J. G. Power, M. Conde, W. Gai, F. Gao, R. Konecny, W. Liu, Z. Yusof, Ph Piot, and M. Rihaoui, in *Proc. PAC'07*, Albuquerque, USA, 2007, pp. 4393-4395.

[6] J. Power, M. Conde, W. Gai, W. Liu, and P. Piot. in *Proc. PAC'09*, Vancouver, Canada,2009, paper TH5RFP005, pp.3444-3446.

[7] M.E. Conde, *et al.,* in *Proc. IPAC'10*, pp. 4310-4312.

[8] A. Halavanau, G. Ha, G. Qiang, W. Gai, J. Power, P. Piot, E. Wisniewski, D. Edstrom, J. Ruan, and J. Santucci, report FERMILAB-TM-2634-APC, 2016.

ISBN 978-3-95450-182-3